One-photon resonant two-photon excitation of Rydberg series close to threshold

G. Alber and Th. Haslwanter

Institute for Theoretical Physics, University of Innsbruck, Innsbruck, Austria

P. Zoller

Joint Institute for Laboratory Astrophysics, University of Colorado and National Bureau of Standards, Boulder, Colorado 80309-0440

Received May 23, 1988; accepted July 18, 1988

We study one-photon resonant two-photon excitation of autoionizing Rydberg series close to threshold. Analytical expressions for the time evolution of bound-state amplitudes are derived by adapting ideas from quantum-defect theory. We discuss in detail the two limiting cases of excitation of Rydberg wave packets and ac-Stark splitting close to the threshold.

1. INTRODUCTION

In a recent series of papers we developed a general theory of laser excitation of Rydberg states close to the ionization threshold.[1,2] Our approach is based on the observation that the laser interaction with Rydberg electrons can be formulated as a finite-range interaction coupling Coulomb-type dissociation channels of the atom laser-field system. Physically this corresponds to the fact that an atom absorbs optical photons in an interaction volume much smaller than the typical size of a Rydberg orbit. In particular this permits ideas from quantum-defect theory[3] to be applied to this problem, with the specific feature that the interaction of the laser with the Rydberg series is treated as a whole; this is opposed to familiar two-level-type theories, which require each of the infinite number of bound (and continuum) states to be explicitly included in a calculation. Furthermore, quantum-defect theory permits an essentially analytical treatment of these laser interactions.

In a previous paper we discussed in some detail one-photon excitation close to a Rydberg threshold by an intense (long) laser pulse.[1] One of the central results of that work was that radial electronic Rydberg wave packets (RWP's) are generated whenever the depletion time of the initial bound state owing to laser-induced transitions to the excited states is less than the classical orbit time of the excited Rydberg electron. We emphasize that this is in contrast to the excitation of RWP's by short pulses, for which the laser-pulse duration has to be shorter than the classical orbit time of the Rydberg electron.[4]

In the present paper we extend this work to one-photon resonant two-photon excitation of autoionizing Rydberg states. We assume that a first laser induces a transition to a resonant intermediate state, from which the electrons are excited by a second laser close to a Rydberg threshold (see Fig. 1). In particular, we will be interested in two limiting cases. First, when the time scale of the laser-induced depletion of the bound states is much shorter than the orbit time of the Rydberg electron, we again find that RWP's are generated. If the two bound states are strongly coupled by the light so that we have ac-Stark splitting (i.e., there are Rabi oscillations in the time evolution of the low-lying bound states), two interfering RWP's are excited, with different orbit times corresponding to transitions from the two ac-Stark split bound states. The second case of interest to be studied below is ac-Stark splitting of a Rydberg series.[5] This occurs when the first laser is weak and the second laser strongly mixes the (intermediate) resonant state into the Rydberg series, i.e., the "excited bound state plus one photon from the second laser" is nearly degenerate and strongly coupled to a large number of Rydberg levels, which is an obvious generalization of the familiar ac-Stark splitting between two resonantly coupled bound states. The structure of this strongly perturbed Rydberg series can be probed as a function of the detuning of the weak first laser. In this limit the time scale of depletion of the ground state is assumed to be much longer than the orbit time of the Rydberg states.

The paper is organized as follows: In Section 2 we derive a dressed-state representation and multiple-scattering expansion for the time evolution of the bound-state amplitudes. In Section 3 we discuss numerical examples of the generation of RWP's and ac-Stark splitting.

2. BASIC EQUATIONS

We consider the process of one-photon resonant two-photon excitation of an autoionizing Rydberg series, as schematically shown in Fig. 1. A laser of frequency ω_1, polarization $\mathbf{e}_1$, and amplitude $\mathcal{E}_1$ induces a resonant transition in the atom from the ground state $|g\rangle$ to the (low-lying) bound state $|e\rangle$. The energies of these levels are denoted by ϵ_g and ϵ_e, respectively (all energies below will be expressed in atomic units). A second laser with frequency ω_2, polarization $\mathbf{e}_2$, and laser amplitude $\mathcal{E}_2$ subsequently excites the atom to autoionizing states close to threshold. For simplicity, we assume that the

0740-3224/88/122439-07$02.00

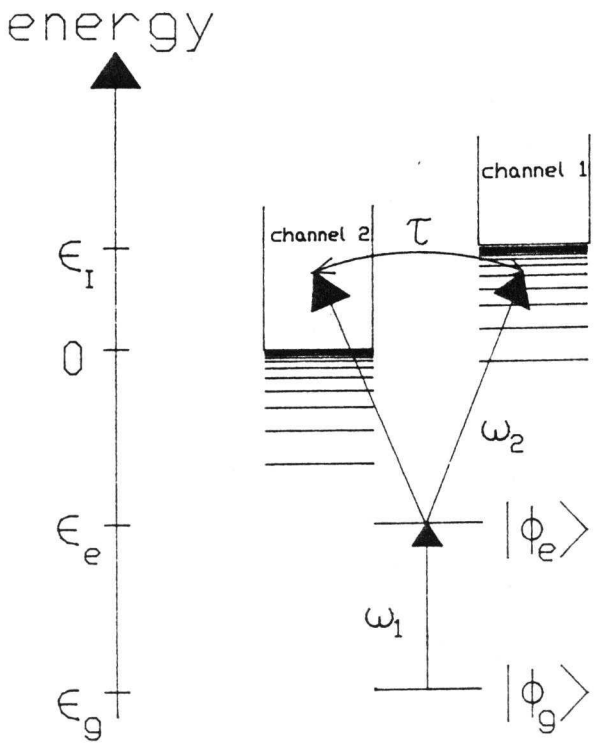

Fig. 1. Schematic representation of the excitation process.

autoionizing series is described within a two-channel model.[3] The thresholds of the first and second channels are denoted by $E_2 = 0$ and $E_1 = \epsilon_I > 0$, respectively. Thus we have for the total energy $E = E_i + \epsilon_i$ $(i = 1, 2)$, where ϵ_i is the energy of the Rydberg electron in channel i. Autoionizing states correspond to Rydberg resonances in the first channel with energy $0 < \epsilon < \epsilon_I$, which can decay into the second channel. Following Seaton,[3] we parameterize the 2×2 electron-ion scattering matrix χ_{ff} (free–free scattering matrix) above both thresholds by

$$\chi_{11} = \frac{1-\tau}{1+\tau}\exp(2\pi i\alpha),$$

$$\chi_{22} = \frac{1-\tau}{1+\tau}\exp(2\pi i\delta),$$

$$\chi_{12} = \chi_{21} = \frac{2i\sqrt{\tau}}{1+\tau}\exp[i\pi(\alpha+\delta)], \tag{1}$$

where $\pi\alpha$ and $\pi\delta$ are continuum phase shifts and τ is a measure of the channel mixing. Dipole-interaction matrix elements for photoionization from the excited state $|e\rangle$ to the first and second channels are denoted by $D^{(-)}_{\epsilon_1 e}$ and $D^{(-)}_{\epsilon_2 e}$, respectively. These matrix elements are proportional to the amplitude $\mathcal{E}_2$. In general the $D^{(-)}$ are complex and can be expressed in terms of real (standing-wave) dipole elements $D_{\epsilon_1 e}$ and $D_{\epsilon_2 e}$ according to[3]

$$D^{(-)}_{\epsilon_1 e} = -ie^{i\pi\alpha}(D_{\epsilon_1 e} + i\sqrt{\tau}D_{\epsilon_2 e})/(1+\tau),$$
$$D^{(-)}_{\epsilon_2 e} = -ie^{i\pi\delta}(D_{\epsilon_2 e} + i\sqrt{\tau}D_{\epsilon_1 e})/(1+\tau). \tag{2}$$

A Fano q parameter is defined as $q = -D_{\epsilon_1 e}/\sqrt{\tau}D_{\epsilon_2 e}$. The interaction matrix element for the bound–bound transition is $D_{eg} = -\langle e|\mathbf{d}\cdot\mathbf{e}_1|g\rangle\mathcal{E}_1$; $\Omega_{eg} = 2|D_{eg}|$ is the corresponding Rabi frequency.

In our model the atomic wave function can be expanded according to

$$|\psi(t)\rangle = |g\rangle a_g(t) + |e\rangle a_e(t) + \sum_{j=1,2}|F_j(t)\rangle. \tag{3}$$

The first two terms correspond to excitation of the bound states $|g\rangle$ and $|e\rangle$ (bound channels). The state vectors $|F_j(t)\rangle$ $(j = 1, 2)$ describe the time evolution of the atomic electrons in the first and second channels (free channels). In configuration space $|F_j(t)\rangle$ is represented by

$$F_j(x, t) = \phi_j(\Omega)F^{(j)}(\rho, t)/\rho. \tag{4}$$

Here x denotes the collection of spin-space coordinates of all atomic electrons, $\phi_j(\Omega)$ is a channel function that characterizes the state of the ionic core (including the angular momentum part of the Rydberg electron), and $F^{(j)}(\rho, t)$ is the time-dependent radial function of the excited Rydberg electron. In what follows we assume that the channel functions $\phi_j(\Omega)$ and the bound states $|g\rangle$ and $|e\rangle$ are mutually orthogonal. Inserting the ansatz (3) into the Schrödinger equation for the many-electron atom in the two laser fields, we find an equation for the time evolution of the amplitudes $a_g(t)$ and $a_e(t)$ and the wave functions $F^{(j)}(\rho, t)$. When the dipole and rotating-wave approximation are used and when the lasers are assumed to be turned on instantaneously at $t = 0$, the Laplace transform of this equation gives a system of close-coupling equations[3] of the form

$$(\epsilon - H_{bb})a(\epsilon) + \int_0^\infty d\rho D_{fb}^{\dagger}(\rho)F(\rho, \epsilon) = iJ, \tag{5a}$$

$$(\epsilon - H_{ff})F(\rho, \epsilon) + D_{fb}(\rho)a(\epsilon) = 0, \tag{5b}$$

with

$$a(\epsilon) = \begin{bmatrix} a_g(\epsilon - \omega_1 - \omega_2) \\ a_e(\epsilon - \omega_2) \end{bmatrix} \tag{6}$$

and

$$F(\rho, \epsilon) = \begin{bmatrix} F^{(1)}(\rho, \epsilon) \\ F^{(2)}(\rho, \epsilon) \end{bmatrix} \tag{7}$$

being the Laplace-transformed amplitudes and radial wave functions, respectively. The Laplace transformation of, e.g., $a_g(t)$ is defined by

$$a_g(z) = \int_0^\infty dt e^{izt}a_g(t) \qquad (z = \epsilon - \omega_1 - \omega_2), \tag{8}$$

with similar definitions for the other quantities. The vector

$$J = \begin{bmatrix} 1 \\ 0 \end{bmatrix} \tag{9}$$

in Eq. (5) incorporates the initial condition $|\psi(t = 0)\rangle = |g\rangle$. The 2×2 bound–bound Hamiltonian matrix

$$H_{bb} = \begin{bmatrix} \bar{\epsilon} & -D_{eg} \\ -D_{eg} & \bar{\epsilon} \end{bmatrix}, \tag{10}$$

with $\bar{\epsilon} = \epsilon_g + \omega_1 + \omega_2$ and $\bar{\epsilon} = \epsilon_e + \omega_2$, describes the laser-induced coupling between the bound states $|g\rangle$ and $|e\rangle$. The 2×2 free–free matrix Hamilton operator

$$H_{\mathrm{ff}} = \begin{bmatrix} \epsilon_I + h_A{}^{(1)}(\rho) & V_{12}(\rho) \\ V_{12}(\rho) & h_A{}^{(2)}(\rho) \end{bmatrix} \tag{11}$$

characterizes the atomic dynamics of the electron in the excited free channels, including configuration interaction. $h_A{}^{(j)}(\rho)$ is the radial part of the atomic Hamiltonian in channel j ($j = 1, 2$), and $V_{12}(\rho)$ is the electrostatic potential responsible for the mixing between the channels. $D_{\mathrm{fb}}(\rho)$ is a (real) 2×2 matrix

$$D_{\mathrm{fb}}(\rho) = \begin{bmatrix} D_{\epsilon_1 g}(\rho) & D_{\epsilon_1 e}(\rho) \\ D_{\epsilon_2 g}(\rho) & D_{\epsilon_2 e}(\rho) \end{bmatrix}, \tag{12}$$

whose matrix elements are defined by

$$D_{\epsilon_i g}(\rho) = 0 \qquad (i = 1, 2),$$

$$D_{\epsilon_i e}(\rho) = \rho \int \mathrm{d}\Omega \phi_i{}^*(\Omega) \mathbf{d} \cdot \mathbf{e}_2 \mathcal{E}_2 \langle x | e \rangle \qquad (i = 1, 2) \tag{13}$$

and correspond to the laser-induced coupling between the bound states $|g\rangle$ and $|e\rangle$ and the free channels $i = 1$ and $i = 2$. We have adopted a matrix notation in Eq. (5) to emphasize that our results are easily generalized to systems with more than two bound states and two free channels.

Equation (5b) is a system of close-coupling equations for the radial wave functions $F(\rho, \epsilon)$, which is coupled to Eq. (5a) for the Laplace-transformed bound-state amplitudes $a(\epsilon)$. It is well known that the non-Coulomb part of the atomic potentials $V_{ij}(\rho)$, which reflects the complicated many-electron interaction in the core region, is restricted to a finite reaction zone (with a typical size of a few Bohr radii). Outside this interaction volume the potential is essentially Coulombic [$V_{ij}(\rho) \simeq -(1/\rho)\delta_{ij} (\rho \geq \rho_0)$]. In addition, because of the localization of the bound states, we have $D_{\epsilon_i e}(\rho) \simeq 0$ for $\rho \geq \rho_0$. This localization of atomic configuration interaction and laser-induced couplings to a finite reaction zone $\rho \leq \rho_0$ permits quantum-defect theory to be applied to solve Eqs. (5). Following the methods outlined in Ref. 1, we find for the Laplace-transformed atomic probability amplitudes that

$$a(\epsilon) = [\epsilon - H_{\mathrm{bb}} - \Sigma_{\mathrm{bb}}(\epsilon)]^{-1} i J, \tag{14}$$

with Σ_{bb} a 2×2 self-energy matrix:

$$\Sigma_{\mathrm{bb}}(\epsilon) = \begin{cases} \Sigma_{\mathrm{bb}}^{(s)} & (\epsilon_I < \epsilon) \\ \Sigma_{\mathrm{bb}}^{(s)} - 2\pi i D_{cb}^{(-)^T} [\chi_{cc} - \exp(-2\pi i \nu_c)]^{-1} D_{cb}^{(-)} & (0 < \epsilon < \epsilon_I) \end{cases}. \tag{15}$$

The self-energy matrix above both thresholds ($0 < \epsilon_I < \epsilon$) is denoted by $\Sigma_{\mathrm{bb}}^{(s)}$. This corresponds to a situation when the second laser ionizes level $|e\rangle$ to the continua in channels 1 and 2. The superscript (s) indicates that it is a smooth function of energy. Explicitly, $\Sigma_{\mathrm{bb}}{}^{(s)}$ is given by

$$\Sigma_{\mathrm{bb}}^{(s)} = \begin{bmatrix} 0 & 0 \\ 0 & \delta\omega - i\tfrac{1}{2}\Gamma \end{bmatrix}, \tag{16}$$

with $\delta\omega$ a quadratic Stark shift (which can be absorbed in a renormalized transition frequency) and Γ is the total ionization rate of level $|e\rangle$:

$$\Gamma = 2\pi \sum_{j=1,2} |D_{\epsilon_j e}^{(-)}|^2. \tag{17}$$

$D_{\epsilon_j e}^{(-)}$ ($j = 1, 2$) is the photoionization dipole matrix element from $|e\rangle$ to the first and second channels defined in Eqs. (2). We have

$$D_{\mathrm{fb}}^{(-)} = \begin{bmatrix} D_{\epsilon_1 g}^{(-)} & D_{\epsilon_1 e}^{(-)} \\ D_{\epsilon_2 g}^{(-)} & D_{\epsilon_2 e}^{(-)} \end{bmatrix}, \tag{18}$$

with[3]

$$D_{\mathrm{fb}}^{(-)} = \int_0^\infty \mathrm{d}\rho F_{\mathrm{ff}}^{(-)}(\rho, \epsilon)^\dagger D_{\mathrm{fb}}(\rho), \tag{19}$$

where $F_{\mathrm{ff}}^{(-)}(\rho, \epsilon)$ is the 2×2 matrix of linearly independent (regular) solutions of the homogeneous part of the close-coupling equation (5b) with boundary conditions appropriate to photoionization [compare Eqs. (2)]. We emphasize that $\Sigma_{\mathrm{bb}}^{(s)}$, $D_{\mathrm{fb}}^{(-)}$, and χ_{ff} are approximately energy independent across the Rydberg threshold. This is a consequence of the finite range of the non-Coulomb interactions in Eqs. (5).

Below threshold, in the autoionizing region $0 < \epsilon < \epsilon_I$, the self-energy is obtained according to Eq. (15) as the sum of a background term $\Sigma_{\mathrm{bb}}^{(s)}$ (smoothly extrapolated from the energy region above threshold) and a resonant term, which shows a rapid variation as a function of energy.[1] The subscript c in Eq. (15) indicates the restriction of indices to the closed channels: in the two-channel problem (Fig. 1) we have

$$D_{cb}^{(-)} = (D_{\epsilon_1 g}^{(-)}, D_{\epsilon_2 e}^{(-)}) = (0, D_{\epsilon_2 e}^{(-)}),$$

$$\chi_{cc} \equiv \chi_{11} = \exp[2\pi i(\alpha + i\beta)] \qquad (\tanh \pi\beta = \tau), \tag{20}$$

and $\nu_c \equiv \nu_1$, the effective quantum number in the first channel [$\epsilon = \epsilon_I - 1/(2\nu_1{}^2)$]. Note that the resonant term has poles at energies corresponding to $\nu_1 = n - \alpha - i\beta$ (n integer), i.e., $\alpha + i\beta$ is the complex quantum defect of the autoionizing Rydberg series. The analytical separation of slowly energy-dependent quantities from resonant terms in the self-energy $\Sigma_{\mathrm{bb}}(\epsilon)$ [Eq. (15)] is of central importance for the following inversion of the Laplace integrals to obtain the time evolution of the atomic wave function.

The time evolution of the bound-state amplitudes,

$$a(t) = \frac{1}{2\pi} \int_{-\infty+i\eta}^{+\infty+i\eta} \mathrm{d}\epsilon \exp[-i(\epsilon - \omega_1 - \omega_2)t] a(\epsilon) \qquad (\eta \to 0^+), \tag{21}$$

with

$$a(t) = \begin{bmatrix} a_g(t) \\ a_e(t) \exp(i\omega_1 t) \end{bmatrix},$$

can be obtained in two alternative but equivalent forms, namely, in a dressed-state representation and in terms of a multiple-scattering expansion.

Performing the integration in Eq. (21) with the help of the residue theorem, we obtain the dressed-state representation

$$a(t) = \sum_n \exp[-i(\tilde{\epsilon}_n - \omega_1 - \omega_2)t]$$
$$\times \left\{\frac{d}{d\epsilon}[\epsilon - H_{bb} - \Sigma_{bb}(\epsilon)]\right\}^{-1}_{\epsilon=\tilde{\epsilon}_n} J$$
$$+ \frac{1}{2\pi}\int_{\epsilon_I+i\eta}^{\infty+i\eta} d\epsilon \exp[-i(\epsilon - \omega_1 - \omega_2)t]$$
$$\times [\epsilon - H_{bb} - \Sigma_{bb}(\epsilon)]^{-1} iJ$$
$$+ \frac{1}{2\pi}\int_{\epsilon_I-i\infty}^{\epsilon_I+i\eta} d\epsilon \exp[-i(\epsilon - \omega_1 - \omega_2)t]$$
$$\times [\epsilon - H_{bb} - \Sigma_{bb}(\epsilon)]^{-1} iJ. \quad (22)$$

Equation (22) expresses $a(t)$ in terms of a sum over dressed states of the atom-field system. The dressed energies are determined by the requirement that

$$\det[\tilde{\chi}_{cc}(\tilde{\epsilon}_n) - \exp(-i2\pi\tilde{\nu}_n)] = 0, \quad (23)$$

with $\tilde{\epsilon}_n = \epsilon_I - 1/(2\tilde{\nu}_n^2)$ and n labeling the different solutions. The 2×2 matrix $\tilde{\chi}_{ff}$ is defined as a scattering matrix of the electron-ion scattering complex,

$$\tilde{\chi}_{ff}(\epsilon) = \chi_{ff} + 2\pi i D_{fb}^{(-)}[\epsilon - H_{bb} - \Sigma_{bb}^{(s)}]^{-1} D_{fb}^{(-)^T}, \quad (24)$$

where the second resonant term is due to laser-induced transitions from the free channels to the bound states $|g\rangle$ and $|e\rangle$. In Eq. (23) the submatrix $\tilde{\chi}_{cc} = \chi_{11}$ again refers to the closed channel 1.

For two channels Eq. (23) can be rewritten in the form

$$(\tilde{\epsilon}_n - \bar{\epsilon})\left[\tilde{\epsilon}_n - \bar{\epsilon} - \gamma_2 \frac{\tau q}{1+\tau} + i\frac{1}{2}\gamma_2 - \frac{1}{2}\gamma_2 \frac{(q-i)^2}{\tan \pi(\tilde{\nu}_n + \alpha)/\tau + i}\right] - \left(\frac{1}{2}\Omega_{eg}\right)^2 = 0, \quad (25)$$

which is a transcendental equation for the dressed-state energies $\tilde{\epsilon}_n$. $\gamma_2 = 2\pi|D_{\epsilon_2 e}|^2$ is the ionization rate of level $|e\rangle$ to the second channel. Close to the threshold, an explicit summation over many dressed states that contribute in Eq. (22) becomes impractical. Instead we can expand $a(t)$, using the results of Ref. 1, into a multiple-scattering series:

$$a(t) = \frac{1}{2\pi}\int_{-\infty+i\eta}^{+\infty+i\eta} d\epsilon \exp[-i(\epsilon - \omega_1 - \omega_2)t]$$
$$\times i[\epsilon - H_{bb} - \Sigma_{bb}^{(s)}]^{-1} J$$
$$+ \sum_{m=0}^{\infty}\int_{-\infty}^{\epsilon_I} d\epsilon \exp[-i(\epsilon - \omega_1 - \omega_2)t]\{i[\epsilon - H_{bb}$$
$$- \Sigma_{bb}^{(s)}]^{-1} D_{cb}^{(-)^T}\}\exp(2\pi i\nu_c)[\tilde{\chi}_{cc}(\epsilon)\exp(2\pi i\nu_c)]^m$$
$$\times \{D_{cb}^{(-)} i[\epsilon - H_{bb} - \Sigma_{bb}^{(s)}]^{-1}\} J, \quad (26)$$

which expresses the atomic probability amplitudes as a sum over contributions of classical trajectories. $m = 0, 1, 2, \ldots$ counts the number of returns of the (classical) electron to the core region.

The dressed-state representation [Eq. (22)] and the multiple-scattering expansion [Eq. (26)] are the central results of this paper. Numerical examples and a physical discussion of Eqs. (22) and (26) will be given in Section 3. Specializing to excitation far above threshold reduces Eq. (22) to results first given by Beers and Armstrong[6] for one-photon resonant two-photon ionization. When the second laser excites only a single isolated Rydberg resonance, Eq. (26) simplifies to equations discussed in Refs. 7 and 8 in the context of strong-field excitation of autoionizing resonances (for details regarding this reduction to an effective three-level system, see Appendix A).

3. RESULTS AND DISCUSSION

In this section we discuss the dynamics of one-photon resonant two-photon excitation of Rydberg series (Fig. 1) on the basis of the dressed-state representation [Eq. (22)] and multiple-scattering expansion [Eq. (26)] for the amplitudes of the bound states $|g\rangle$ and $|e\rangle$. This process is characterized by the following parameters: Ω_{eg} and $\Delta = \omega_1 - (\epsilon_e - \epsilon_g) = \tilde{\epsilon} - \bar{\epsilon}$, which are the Rabi frequency and detuning for the first excitation step $|g\rangle - |e\rangle$, respectively; Γ, the total ionization rate of level $|e\rangle$, which is a measure of laser-induced coupling between $|e\rangle$ and the Rydberg series, and the corresponding Fano q parameter; $\Delta\epsilon_n = (n - \alpha)^{-3}$, the level spacing between adjacent Rydberg states; and α and τ, the quantum defect in the first channel and the channel mixing parameter, respectively. Depending on the relative values of these parameters, we distinguish between different limiting cases, which are discussed in what follows.

A. Excitation of Rydberg Wave Packets

Here we study situations below the threshold ϵ_I, where many dressed states contribute to the sum in Eq. (22) for $|a_g(t)|^2$ and $|a_e(t)|^2$. In this case a qualitative physical picture of the dynamics of the excitation process is obtained from the multiple-scattering expansion.

The non-Hermitian Hamilton matrix $H_{bb} + \Sigma_{bb}^{(s)}$ has eigenvalues

$$\lambda^{(1,2)} = \tfrac{1}{2}(\bar{\epsilon} + \tilde{\epsilon} - i\tfrac{1}{2}\Gamma) \pm \tfrac{1}{2}[(\bar{\epsilon} - \tilde{\epsilon} - i\tfrac{1}{2}\Gamma)^2 + \Omega_{eg}^2]^{1/2}. \quad (27)$$

Its right (left) eigenvectors $A_{jr}(B_{rj})(r = 1, 2; j = e, g)$ are given by

$$A = \begin{bmatrix} \tfrac{1}{2}\Omega_{eg} & \tfrac{1}{2}\Omega_{eg} \\ \tilde{\epsilon} - \lambda^{(1)} & \tilde{\epsilon} - \lambda^{(2)} \end{bmatrix},$$
$$B = A^{-1}. \quad (28)$$

Physically $H_{bb} + \Sigma_{bb}^{(s)}$ describes the time evolution of one-photon resonant two-photon excitation above both thresholds. In terms of these eigenvectors and eigenvalues, the multiple-scattering expansion of Eq. (26) reads as

$$a_i(t) = \sum_{r=1,2} \exp\{-i[\lambda^{(r)} - \omega_1 - \omega_2]t\} A_{ir} B_{rg}$$
$$+ \sum_{r,r'=1,2}\sum_{m=0}^{\infty}\int_{-\infty}^{\epsilon_I} d\epsilon \exp[-i(\epsilon - \omega_1 - \omega_2)t] A_{ir}$$
$$\times \frac{i}{\epsilon - \lambda^{(r)}} B_{re} D_{1e}^{(-)} \exp(i2\pi\nu_1)[\tilde{\chi}_{11}(\epsilon)\exp(2i\pi\nu_1)]^m$$
$$\times D_{1e}^{(-)} A_{er'} \frac{i}{\epsilon - \lambda^{(r')}} B_{r'g} \qquad (i = e, g), \quad (29)$$

with $\nu_1 = [2(\epsilon_I - \epsilon)]^{-1/2}$. In the present case of interest,

$\exp(2\pi i\nu_1)$ is a rapidly oscillating function of energy in comparison with the rest of the integrand. This assumes that the imaginary parts of $\lambda^{(r)}$ $(r = 1, 2)$ [Eq. (27)] (which roughly characterize the scale of the energy variation of the nonoscillating part of the integrand) are much larger than the level spacing of the Rydberg states. This corresponds to excitation close to the photoionization threshold. Under these conditions we can perform the energy integration in Eq. (29) with the method of stationary phase. The dominant contribution at time t then comes from energies $\epsilon_s(m, t)$, determined by

$$t = mT_{\epsilon_s(m,t)} \qquad (m = 1, 2, \ldots), \tag{30}$$

with $T_\epsilon = 2\pi[2(\epsilon_I - \epsilon)]^{-3/2}$ the classical orbit time of the Rydberg electron with energy ϵ in the first channel.

This suggests the following physical picture of the excitation process: The condition that $\exp(i2\pi\nu_1)$ is a rapidly oscillating function of energy implies that the initially occupied atomic state $|g\rangle$ is depleted on a time scale that is short in comparison with the classical orbit times associated with the significantly excited autoionizing Rydberg states. The laser-induced excitation process is therefore localized not only in space (see the discussion in Section 2) but also in time, so a localized RWP is generated. For times much shorter than the classical orbit time of significantly excited Rydberg states, this wave packet has not yet "seen" the outer turning point of the Coulomb potential due to the ionic core and therefore behaves as in an ionization process. This is reflected by the first term in Eq. (29), which gives the dominant contribution to $a_i(t)$ for these times and consists of a linear combination of exponentially decaying terms that we would obtain in the case of a one-photon resonant two-photon ionization process in an energy range above both thresholds.[6] Eventually the RWP is reflected at the outer turning point of its orbit and returns to the ionic core. With each return either it is deexcited into one of the bound atomic states by a stimulated recombination process or it experiences a laser-assisted electron-ion scattering process and leaves the core region again.

This physical picture of the excitation process close to threshold manifests itself in the time evolution of the bound-state probability amplitudes. Figure 2 shows $|a_g(t)|^2$ as a function of the interaction time between the atom and the laser fields in the case of one-photon resonant two-photon excitation of a Rydberg series of bound states for $\Delta = 0$ and different mean excited energies $\bar{\epsilon}$. The Rabi frequency of the first laser Ω_{eg} is assumed to be much larger than Γ, which characterizes the strength of the laser-induced transition between $|e\rangle$ and the bound Rydberg states. In this case we find from Eq. (27) that

$$\lambda^{(1,2)} = \bar{\epsilon} \pm \frac{1}{2}\,\Omega_{eg} - i\,\frac{\Gamma}{4}, \tag{31}$$

which reflects the ac-Stark splitting associated with the strongly coupled transition $|g\rangle \rightarrow |e\rangle$. In Fig. 2(a) the depletion time $1/\Gamma$ of the initially occupied state $|g\rangle$ is comparable with the classical orbit time of the significantly excited states $T_{\bar{\epsilon}}$. The excitation process is therefore not well localized in time, and the time dependence of $|a_g(t)|^2$ is rather complicated. In Fig. 2(b) we are exciting Rydberg states closer to the Rydberg threshold so that $1/\Gamma \ll T_{\bar{\epsilon}}$. We notice the characteristic time dependence, which reflects the generation of a RWP. For times $t \ll T_{\bar{\epsilon}}$, $|a_g(t)|^2$ exhibits exponentially decaying Rabi oscillations, which is typical for one-photon resonant two-photon ionization. Because $|\Omega_{eg}| \gg \Gamma$, two RWP's with energies $\epsilon = \bar{\epsilon} \pm \frac{1}{2}\Omega_{eg}$ are generated by the excitation process [see Eq. (31)]. At time $t \approx T_{\bar{\epsilon}-1/2\Omega_{eg}}$ the faster wave packet has returned to the core region, giving rise to an increase of $|a_g(t)|^2$, which is due to stimulated recombination of the disintegrated electron–ion complex. For the parameters chosen in Fig. 2(b), we have $T_{\bar{\epsilon}+1/2\Omega_{eg}} \approx 2T_{\bar{\epsilon}-1/2\Omega_{eg}}$, so that the faster wave packet overlaps with the slower wave packet in the core region at $t \approx 2T_{\bar{\epsilon}-1/2\Omega_{eg}}$. This manifests itself in quantum-mechanical interferences between the recombination amplitudes, which determine $|a_g(t)|^2$.

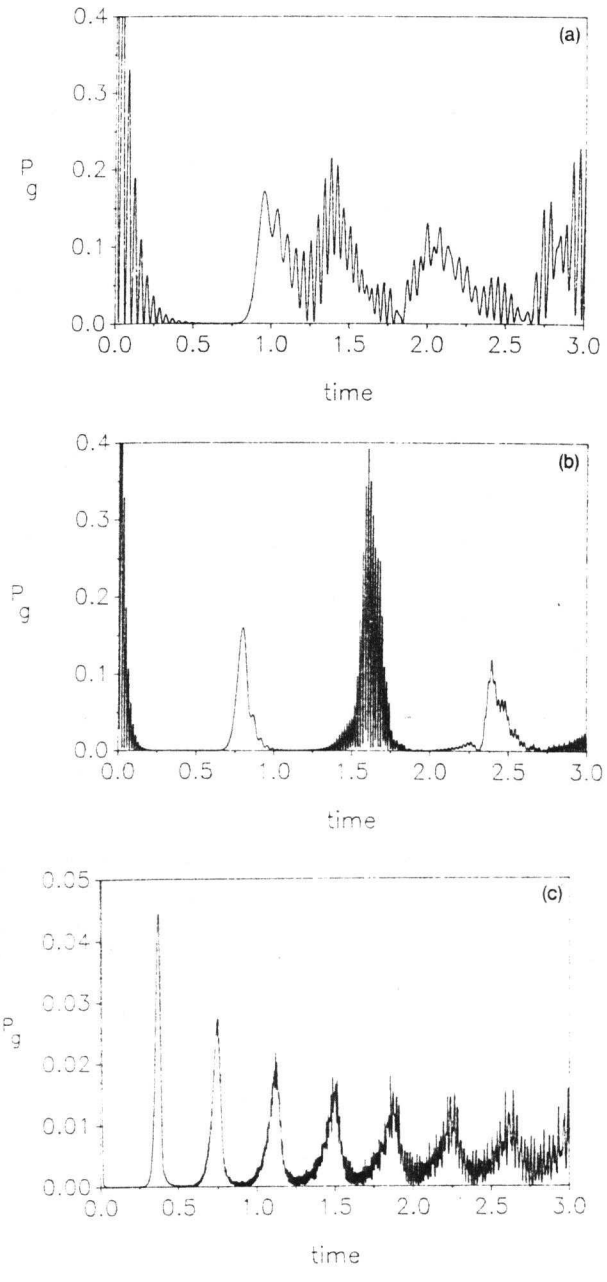

Fig. 2. Ground-state probability as a function of time (in units of $T_{\bar{\epsilon}}$) in the case of excitation of a Rydberg series of bound states for $\Omega_{eg} = 4 \times 10^{-6}$, $\Gamma = 7 \times 10^{-7}$, $\Delta = 0$, $\alpha = 0$, and (a) $\bar{\epsilon} = -1.5 \times 10^{-5}$, (b) $\bar{\epsilon} = -8 \times 10^{-6}$, (c) $\bar{\epsilon} = -2 \times 10^{-6}$.

In Fig. 2(c) we are exciting Rydberg states so close to threshold that $T_{\tilde{\imath}+1/2\Omega_{eg}} \gg T_{\tilde{\imath}-1/2\Omega_{eg}}$. Correspondingly, before the slow RWP has significantly moved away from the reaction zone the fast RWP has already had enough time to return to the core region many times. The recombination peaks in Fig. 2(c) are due therefore only to successive returns of the fast wave packet. We also notice small interference effects, which are due to the overlap between both wave packets inside the reaction zone.

We emphasize that the above discussion rests on the assumption of rectangular laser pulse envelopes. When the first laser is turned on adiabatically, only a single dressed state of the bound–bound transition is populated, and only one wave packet is generated.

B. Ac-Stark Splitting of a Rydberg Series

If we are exciting Rydberg states sufficiently far below the Rydberg threshold, only a few dressed states contribute to the atomic transition amplitudes, which are therefore most conveniently expressed in terms of the dressed-state representation [see Eq. (22)]. In Appendix A we show that in the limit where $\tau \ll 1$ and where $\max\{|\Delta|, \Omega_{eg}, \Gamma, \Omega_{eg}{}^2/\Gamma\} \ll \Delta_{\epsilon_n}$, only the autoionizing state with energy $\epsilon_n = \epsilon_I - 1/2(n-\alpha)^{-2}$ is dominantly excited, and the dressed-state representation reduces to the results that were previously obtained in Refs. 7 and 8. In particular, these studies show that by using a weak first laser pulse and by varying its frequency over the atomic transition $|g\rangle \rightarrow |e\rangle$, we can probe the dynamics of an isolated autoionizing resonance, which is strongly coupled to the bound atomic state $|e\rangle$ by our intense second laser field. In this case quantum-mechanical inteferences between amplitudes associated with different excitation paths lead to asymmetric spectra and to the appearance of bound states in the continuum[9] when the configuration interaction and laser-induced couplings are of comparable strength.

With the help of Eq. (22), these results may easily be generalized to cases when the second laser pulse becomes so intense that more than one autoionizing resonance is strongly coupled to $|e\rangle$.[5] For this purpose we use the fact that in the limit $|\Omega_{eg}| \ll \Gamma$ this dominant contribution to the atomic-transition amplitudes comes from the dressed state $\tilde{\epsilon}_1$, which is approximately given by

$$\tilde{\epsilon}_1 = \tilde{\epsilon} + \frac{(\frac{1}{2}\Omega_{eg})^2}{\tilde{\epsilon} - \bar{\epsilon} - \gamma_2 \dfrac{\tau q}{1+\tau} + i\dfrac{\gamma_2}{2} - \dfrac{\gamma_2}{2}\dfrac{(q-i)^2}{\tan \pi(\tilde{\nu}+\alpha)/\tau + i}}. \tag{32}$$

This implies that the initial-state probability $|a_g(t)|^2$ is exponentially decaying with the ionization rate

$$R = -\frac{1}{2}\Omega_{eg}^2 \operatorname{Im}\left[\frac{1}{\tilde{\epsilon} - \bar{\epsilon} - \gamma_2 \dfrac{\tau q}{1+\tau} + i\dfrac{\gamma_2}{2} - \dfrac{\gamma_2}{2}\dfrac{(q-i)^2}{\tan \pi(\tilde{\nu}+\alpha)/\tau + i}}\right], \tag{33}$$

which reduces to the result of Ref. 7 if only one autoionizing resonance is involved in the excitation process.[10] Figures 3(a) and 3(b) show R as a function of ω_1 for a fixed value of ω_2, which was chosen so that the second laser pulse resonantly excites an autoionizing state. The positions of the two

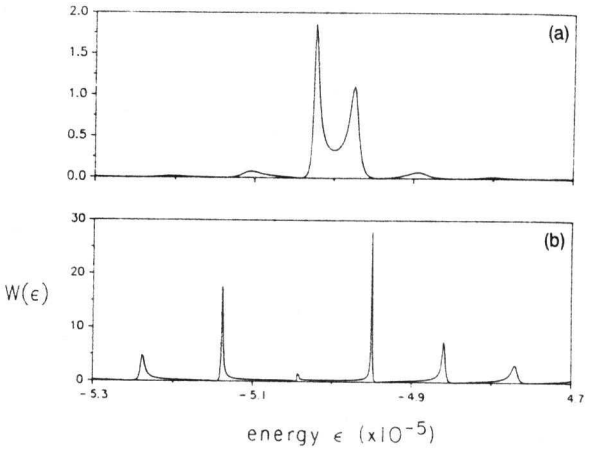

Fig. 3. Ionization rate for fixed ω_1 as a function of energy $\epsilon = \epsilon_g + \omega_1 + \omega_2$ (in units of $\Omega_{eg}{}^2/\Gamma$) for $\bar{\epsilon} = -5 \times 10^{-5}$, $\tau = 0.5$, $q = 10$, $\alpha = 0$, and (a) $\gamma_1 = 5 \times 10^{-7}$, (b) $\gamma_1 = 8 \times 10^{-6}$.

maxima in Fig. 3(a) correspond to the ac-Stark split states associated with the strongly coupled states $|e\rangle$ and $|n\rangle$. The different widths and heights of these two peaks reflect the quantum-mechanical interferences between the direct laser-induced transition $|e\rangle \rightarrow |n\rangle$ and the indirect one through the electron continuum, which also involves the configuration interaction. However, in this figure the intensity of the second laser is already so high that adjacent autoionizing states are also affected by the laser-induced mixing between $|e\rangle$ and channels 1 and 2, which may be recognized by the small side peaks. In Fig. 3(b) the second laser is so intense that many autoionizing Rydberg states are significantly mixed into $|e\rangle$. Correspondingly the ac-Stark splitting is much larger. Furthermore, all resonances experience an additional quadratic Stark shift of magnitude $\gamma_2 \tau q/(1+\tau)$.

4. CONCLUSIONS

In conclusion, we have studied one-photon resonant two-photon excitation of autoionizating Rydberg series close to threshold. We have derived analytical expressions for atomic-transition amplitudes, adapting methods from quantum-defect theory. Whereas the time evolution of the bound-state amplitudes sufficiently below the Rydberg threshold is conveniently expressed in the form of a dressed-state representation, a multiple-scattering expansion is particularly suited to deal with excitation close to threshold.

In this paper we have discussed two limiting cases. In the first case we assume that the time scale of depletion of the low-lying atomic bound states is shorter than the classical orbit time of the Rydberg electron. This leads us to the physical picture of (radial) RWP's moving in the Coulomb potential of the ion core. The second limiting case is one when a first, weak laser introduces a bottleneck in the excitation process and the second laser strongly couples the intermediate resonance to many Rydberg states, corresponding to ac-Stark splitting of a Rydberg series.

APPENDIX A

In this appendix we derive expressions for the atomic-transition amplitudes in the three-level limit when an isolated

autoionizing state is excited. If $\tau \ll 1$ and if $\max\{|\Delta|, \Omega_{eg}, \Gamma, \Omega_{eg}^2/\Gamma\} \ll |\Delta\epsilon_n|$, only the autoionizing state $|n\rangle$ with energy $\epsilon_n = \epsilon_I - \frac{1}{2}(n-\alpha)^{-2}$ is excited. Under these conditions we can expand $\tan \pi(\tilde{\nu}_n + \alpha)$ in Eq. (25) into a Taylor series. Taking only the first two terms, we obtain for the dressed energies the equation

$$(\tilde{\epsilon}_n - \bar{\epsilon})[\tilde{\epsilon}_n - \bar{\epsilon} + i\tfrac{1}{2}\gamma_2 - (\tfrac{1}{2}\tilde{\Omega}_n)^2(1 - i/q)^2/(\tilde{\epsilon}_n - \epsilon_n + i\tfrac{1}{2}\Gamma_n)] - (\tfrac{1}{2}\Omega_{eg})^2 = 0. \quad \text{(A1)}$$

$\Gamma_n = (2\tau/\pi)(n-\alpha)^{-3}$ is the decay rate of the autoionizing state, and $\tilde{\Omega}_n$ is a generalized Rabi frequency describing the laser-induced transitions $|e\rangle \rightarrow |n\rangle$ and is defined by $\tilde{\Omega}_n^2 = \gamma_2\Gamma_n q^2$. The cubic Eq. (A1) determines the three dressed states, which characterize the dynamics of the excitation process. Making the analogous expansions in the resonant part of Eqs. (14) and (15), we obtain for the Laplace-transformed atomic amplitudes

$$a(\epsilon) = \begin{bmatrix} \epsilon - \bar{\epsilon} & D_{eg} \\ D_{eg} & \epsilon - \bar{\epsilon} + i\tfrac{1}{2}\gamma_2 - (\tfrac{1}{2}\tilde{\Omega}_n)^2(1 - i/q)^2/(\epsilon - \epsilon_n + i\tfrac{1}{2}\Gamma_n) \end{bmatrix}^{-1} iJ. \quad \text{(A2)}$$

This result coincides with Eq. (5.17) of Ref. 7, where it was derived by using the resolvent operator formalism.

ACKNOWLEDGMENTS

The research of G. Alber and Th. Haslwanter was supported by the Austrian Science Foundation. P. Zoller, who was a 1988 Visiting Fellow, thanks the Joint Institute for Laboratory Astrophysics for its hospitality.

REFERENCES AND NOTES

1. G. Alber and P. Zoller, Phys. Rev. A **37,** 377 (1988).
2. A. Giusti-Suzor and P. Zoller, Phys. Rev. A **36,** 5178 (1987).
3. M. J. Seaton, Rep. Prog. Phys. **46,** 167 (1983).
4. J. Parker and C. R. Stroud, Jr., Phys. Rev. Lett. **56,** 716 (1986); W. A. Henle, H. Ritsch, and P. Zoller, Phys. Rev. A **36,** 683 (1987); for observation of angular wave packets, see J. A. Yeazell and C. R. Stroud, Jr., Phys. Rev. Lett. **60,** 1494 (1988).
5. G. Alber and P. Zoller, Phys. Rev. A **29** 2290 (1984).
6. B. L. Beers and L. Armstrong, Phys. Rev. A **12,** 2447 (1975).
7. P. Lambropoulos and P. Zoller, Phys. Rev. A **24,** 379 (1981).
8. For reviews and references to early work, see P. Lambropoulos and P. Zoller, in *Multiphoton Ionization of Atoms,* S. L. Chin and P. Lambropoulos, eds. (Academic, New York, 1986) and P. Knight, Comments At. Mol. Phys. **15,** 193 (1984); see also Z. Deng and J. H. Eberly, J. Opt. Soc. Am. B **1,** 102 (1984); A. Lami and N. K. Rahman, Phys. Rev. A **34,** 3908 (1986); H. Bachan, P. Lambropoulos, and R. Shakeshaft, Phys. Rev. A **34,** 4785 (1986); S. Ravi and G. S. Agarwal, Phys. Rev. A **35,** 3291, 3354 (1987); A. Raczynski and J. Zaremba, J. Phys. B **19,** 3895 (1986); J. Phys. B **20,** 1919 (1986); Phys. Rev. A **36,** 5079 (1987).
9. H. Friedrich and D. Wintgen, Phys. Rev. A **31,** 3964 (1985); **32,** 3231 (1985).
10. This result is analogous to weak-field excitation of complex autoionizing resonances; see A. Giusti-Suzor and H. LeFebvre-Brion, Phys. Rev. A **30,** 3057 (1984).